



New hybrid silsesquioxane materials with sterically hindered carbosilane side groups

Anna Kowalewska^{a,*}, Witold Fortuniak^a, Bartosz Handke^b

^a Centre of Molecular and Macromolecular Studies, Polish Academy of Sciences, Sienkiewicza 112, 90-363 Łódź, Poland

^b AGH University of Science and Technology, Faculty of Materials Science and Ceramics, Al. Mickiewicza 30, 30-059 Kraków, Poland

ARTICLE INFO

Article history:

Received 29 October 2008

Received in revised form 11 December 2008

Accepted 12 December 2008

Available online 25 December 2008

Keywords:

Silsesquioxane

Carbosilane

Tris(trimethylsilyl)methane

Hybrid materials

ABSTRACT

Unique silsesquioxane materials, bearing highly sterically hindered carbosilane substituents at SiO_{3/2} centre, were derived from a novel precursor – (Me₃Si)₃CSiMe₂CH₂CH₂Si(OEt)₃ – in a hydrolytic condensation process under nucleophilic catalysis conditions. As proved by analytical results, crystalline or ladder-like [(Me₃Si)₃CSiMe₂CH₂CH₂SiO_{3/2}]_n (PT_{Si}SS) were obtained, depending on the applied reaction conditions. Due to the intrinsic features of (Me₃Si)₃CSiMe₂–carbosilane substituent (the bulk and large amount of Si–C bonds), the obtained ladder-like silsesquioxanes show specific properties (good solubility, low dielectric constant κ).

© 2008 Elsevier B.V. All rights reserved.

1. Introduction

Oligomers and polymers of silsesquioxane framework (POSS) can be typically obtained by hydrolysis of trichloro- or trialkoxysilanes [1]. The steric effect, generated by an organic group at silicon atom of RSiOR'₃ or RSiCl₃, is one of the most important factors directing structure of a growing silsesquioxane molecule. Highest yields of polyhedral, crystalline silsesquioxanes (RSiO_{3/2})₆ [2] or (RSiO_{3/2})₈ [3] were achieved with precursors bearing sterically demanding ligands. On the other hand an ordered structure of polymeric silsesquioxane matrix can be generated by a specific choice of reaction conditions [4] or a “self-template” effect provided by specific morphology of the used precursors [5]. Self-organization and nanostructuring in these hybrid organic–inorganic materials can be also achieved by surfactant-mediated methods [6].

Tris(trimethylsilyl)methyl group (T_{Si}), and its derivatives, are well known for the steric hindrance they can provide [7]. Bulky T_{Si} groups have already been applied in polymeric systems and were shown to exert an exceptional effect on the structure and properties of macromolecules [8]. The unique steric requirements of T_{Si} moiety can be also taken advantage of in the preparation of hybrid carbosilane–silsesquioxane materials. The sheer volume and nonpolarity of (Me₃Si)₃CSiMe₂CH₂CH₂– substituent should provide a “self-template” effect and direct the condensation of alkoxysilyl groups into formation of regular (polyhedral or ladder-

like) structures. The presented work is focused on the relationship between the reaction conditions and the structure of the obtained [(Me₃Si)₃CSiMe₂CH₂CH₂SiO_{3/2}]_n (PT_{Si}SS) materials (analyzed by XRD, NMR and FTIR). Moreover, characteristic properties of PT_{Si}SS were studied by TGA, DSC and permittivity measurements. It was shown that PT_{Si}SS, having an exceptionally high amount of alternating Si–C bonds, are thermally resistant insulating materials.

2. Results and discussion

2.1. Preparation of [(Me₃Si)₃CSiMe₂CH₂CH₂SiO_{3/2}]_n silsesquioxanes

Hybrid carbosilane–silsesquioxane materials, based on Si₈O₁₂ cube, were obtained so far using [NMe₄]₈[Si₈O₂₀] [9], or (HSiO_{3/2})₈, (CH₂=CHSiO_{3/2})₈, (CH₂=CHSiMe₂SiO_{3/2})₈ and (HSiMe₂SiO_{3/2})₈ [10] as respective precursors. Specifically, carbosilane dendrimers having central Si₈O₁₂ unit were prepared by building up the carbosilane arms in consecutive hydrosilylation/vinylation steps [11]. We have chosen the “convergent” approach, and preparation of silsesquioxane molecules surrounded by carbosilane groups, using reactive trialkoxysilane (Me₃Si)₃CSiMe₂CH₂CH₂Si(OEt)₃ as the precursor (Scheme 1).

Condensation of the precursor in a typical acid/base catalyzed sol–gel process was the initial synthetic approach. The first discouraging experiments ended up with mixtures of unreacted (Me₃Si)₃CSiMe₂CH₂CH₂Si(OEt)₃ and short silsesquioxane oligomers (a typical result for sol–gel reactions carried out using trialkoxysilyl monomers with bulky organic substituents [12]). The sol–gel approach was replaced then by hydrolytic condensation catalyzed

* Corresponding author. Tel.: +48 4268 03203; fax: +48 4268 47126.
E-mail address: anko@cbmm.lodz.pl (A. Kowalewska).



Scheme 1. Preparation of [tris(trimethylsilyl)methyl]dimethylsilyl-silsesquioxanes.

by an ionic catalyst – tetrabutylammonium fluoride (TBAF). TBAF was previously successfully used for the preparation of octahedral silsesquioxanes with cyclopentyl or cyclohexyl groups [13], as well as octamethyloctasilsesquioxane [14]. It turned out to be the method of choice for $\text{PT}_{\text{Si}}\text{SS}$ materials, which were obtained with good yields under the applied conditions. Since commercially available TBAF contains about 5% of water, that can be used in the hydrolysis of alkoxy-silyl groups, H_2O itself was not added to the system. The reaction was carried out under very mild conditions, at room temperature, in a variety of solvents [ethanol, acetone, dichloromethane and tetrahydrofuran (Table 1)]. Precipitation of insoluble products was observed for all the studied systems. In EtOH the insoluble fraction I-A was separated (“A” for all experiments throughout the text is a label for the insoluble product), and the soluble residue (fraction I-B) was recovered from the filtrate and purified. In THF and acetone all $\text{PT}_{\text{Si}}\text{SS}$ products precipitated as insoluble fractions (respectively, II-A and IV-A). Insoluble $\text{PT}_{\text{Si}}\text{SS}$ (III-A) precipitated also from CH_2Cl_2 , but in this case the remaining soluble residue was composed of two different type polysilsesquioxanes (fraction III-B – fine particles precipitating after concentration of the filtrate, fraction III-C – fibrous polymer obtained by precipitation of the most soluble part of $\text{PT}_{\text{Si}}\text{SS}$ into EtOH). All $\text{PT}_{\text{Si}}\text{SS}$ products, separated as white solids from the reaction mixture, were still soluble to various degree in organic solvents (THF, CH_2Cl_2 , CHCl_3) after drying.

2.2. Characterization of the structure of hybrid carbosilane–silsesquioxanes

A substantial solvent effect on the structure of $\text{PT}_{\text{Si}}\text{SS}$ material could be anticipated, similar to the one observed for condensation of 2,4,6,8-tetraethoxy-2,4,6,8-tetramethylcyclotetrasiloxanes [14] or $\text{CpSi}(\text{OEt})_3$ [13] in the presence of TBAF. THF is reported to promote formation of highly condensed porous solids (especially in the presence of an ionic catalyst as TBAF), whereas nonporous

xerogels can be obtained in alcohols [15]. Indeed, the kind of reaction medium controls also the structure of $\text{PT}_{\text{Si}}\text{SS}$. The type of structure was evaluated on the basis of results obtained using complementary analytic methods (XRD, NMR, FTIR).

2.2.1. X-ray powder diffraction

It was found that the separated fraction III-A (obtained in CH_2Cl_2) is composed of regular, crystalline polyhedral species (characteristic XRD lines at $2\theta = 5.96^\circ$ and $2\theta = 11.86^\circ$, Fig. 1). Polymeric $\text{PT}_{\text{Si}}\text{SS}$ (I-A, II-A, III-B, III-C and IV-A) show two characteristic broad lines at $2\theta = 5.1^\circ$ and $2\theta = 11.8^\circ$ in their XRD spectra (Fig. 2). These peaks indicate a certain degree of organization in the silsesquioxane framework of $\text{PT}_{\text{Si}}\text{SS}$ materials. In silsesquioxanes two broad Bragg peaks can be an indicator (not a conclusive one) of an ordered ladder-like organization of siloxane bonds [16]. Similar broad XRD patterns were also reported for meso-structured layered POSS materials, built of alternating inorganic and organic phases [17,18]. For example, two broad signals corresponding to 6.4 Å and 15.7 Å spacing, were observed for carboranyl-containing [1,2- $\text{C}_2\text{B}_{10}\text{H}_{10}$ -1,2-($\text{CH}_2\text{CH}_2\text{CH}_2\text{SiO}_{3/2}$) $_2$] $_n$ silsesquioxanes [17]. The materials exhibited a lamellar structure due to periodic alternating organo-carboranyl units and silica layers. XRD halos of polymeric $\text{PT}_{\text{Si}}\text{SS}$ correspond to spacing of 17.3 Å ($2\theta = 5.1^\circ$) and 7.5 Å ($2\theta = 11.8^\circ$). The spacing can be compared to characteristic distances calculated for the proposed arrangement (Scheme 2). The intramolecular chain-to-chain distance [i.e. the width (w) of each double-chained ladder-like molecule] is close to 17.3 Å, whereas the spacing of 7.5 Å indicates the average thickness (t) of the ladder-like polymer. The result (supported by NMR and FTIR data, as well as very good solubility of the obtained materials) suggested that $\text{PT}_{\text{Si}}\text{SS}$ indeed can be of ladder-like structure. A closer look on XRD pattern of II-A revealed that along the ladder-like product also a crystalline form of $\text{PT}_{\text{Si}}\text{SS}$ is present in the sample. Due to their similar solubility in THF, both species precipitated together from the reaction mixture. The XRD diffractogram of the crystalline part of II-A differs slightly from the one recorded for III-A, and is composed of a set of multiple sharp peaks overlapping the XRD pattern of ladder-like material. Bragg peaks in sample IV-A obtained in acetone, also correspond to the ladder-like model, but are more sharp. Thus, as evaluated by XRD, the structure of $\text{PT}_{\text{Si}}\text{SS}$ correlates with the type of solvent used for the reaction. Aprotic solvents of low polarity (CH_2Cl_2 , THF) helped most to the formation of crystalline species. The material of the least regular structure (judging by broadness of its Bragg peaks) was obtained in polar and protic EtOH.

Table 1
Reaction conditions and characteristics of $[(\text{Me}_3\text{Si})_3\text{CSiMe}_2\text{CH}_2\text{CH}_2\text{SiO}_{3/2}]_n$ products.

Sample	Solvent	Type	ϵ	Y	$X_{(\text{OEt})}$	$\delta n/\delta C$	$[C_c]/[C_i]$	Mn_{RI}	PDI_{RI}	Mn_{MALLS}	PDI_{MALLS}	Mn_{RALLS}	PDI_{RALLS}	$[\eta]$	R_h	C	H
I-A	EtOH	p-p	24.0	73.6	97.9	0.142	0.92	1400	1.1	2700	1.0	3300	1.1	0.0258	1.11	41.61	9.93
I-B	EtOH	p-p	24.0	8.4	88.5	–	–	–	–	–	–	–	–	–	–	23.91	6.26
II-A	THF	a	7.5	75.2	93.5	0.100	0.68	1600	1.4	3800	1.2	3900	1.2	0.0281	1.24	41.69	9.80
III-A	CH_2Cl_2	a	9.1	24.1	99.7	0.100	0.12	1300	1.1	3300	1.3	3000	1.2	0.0247	1.09	45.04	10.09
III-B	CH_2Cl_2	a	9.1	15.2	98.5	0.090	0.98	1500	1.2	4400	1.2	3400	1.1	0.0205	1.05	40.61	9.54
III-C	CH_2Cl_2	a	9.1	43.3	98.4	0.100	0.98	1500	1.1	3900	1.0	4200	1.0	0.0229	1.14	44.64	9.45
IV-A	acetone	p-a	37.0	80.1	95.1	0.100	0.58	1400	1.1	4100	1.0	4000	1.1	0.0245	1.17	43.53	9.06

ϵ – dielectric constant of solvent.

Solvent type – a (aprotic), p-a (polar aprotic), p-p (polar protic).

Y – yield (%).

$X_{(\text{OEt})}$ – degree of hydrolysis of alkoxy-silyl groups by ^1H NMR (%).

$\delta n/\delta C$ – refractive index increment (in italics are artificial $\delta n/\delta C$, assumed for less soluble samples on the basis of the value found for III-C).

$[C_c]/[C_i]$ – index of concentration (C_c – calculated by apparatus, C_i – of the prepared solution before filtration).

RI, MALLS, RALLS – detection methods.

$[\eta]$ – intrinsic viscosity (dL/g).

R_h – hydrodynamic radius (nm).

C – amount of carbon found for completely condensed $[(\text{Me}_3\text{Si})_3\text{CSiMe}_2\text{CH}_2\text{CH}_2\text{SiO}_{3/2}]_n$ (wt%) (calculated 45.53%).

H – amount of hydrogen found for completely condensed $[(\text{Me}_3\text{Si})_3\text{CSiMe}_2\text{CH}_2\text{CH}_2\text{SiO}_{3/2}]_n$ (wt%) (calculated 10.03%).

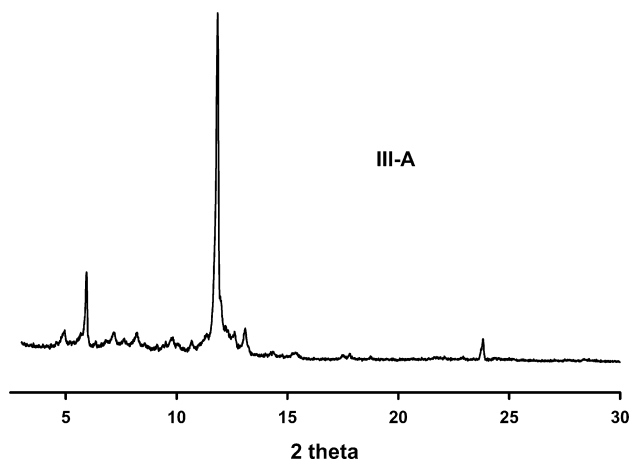


Fig. 1. XRD of crystalline PT_{Si}SS (III-A).

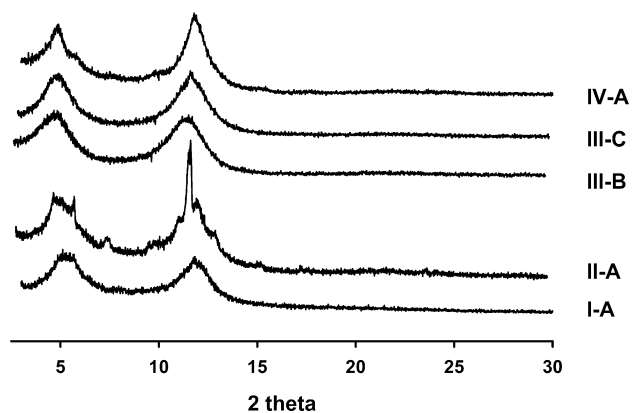
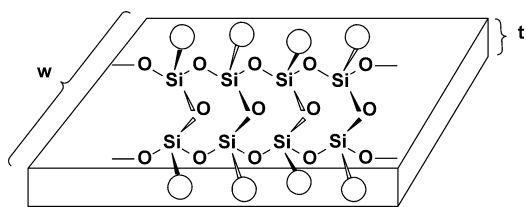


Fig. 2. XRD of ladder-like PT_{Si}SS.



Scheme 2. Proposed ladder-like arrangement in PT_{Si}SS [○ and ● indicate (Me₃Si)₃CSiMe₂CH₂CH₂- substituents, w – width and t – thickness of a silsesquioxane ladder].

2.2.2. NMR study

NMR analysis proved high degree of condensation in the studied PT_{Si}SS samples. ¹H NMR spectra confirmed almost complete hydrolysis of Si–OEt moieties (Table 1). Also only T₃ [T₃: CSi(OSi)₃] type siloxane units were observed in ²⁹Si CP MAS NMR spectra at –65.4 ppm (Fig. 3). No T₀ [T₀: CSi(OR)₃, R = H or Et], T₁ [T₁: CSi(O–Si)(OR)₂] or T₂ [T₂: CSi(OSi)₂OR], (expected at ~–42 ppm, –49 ppm and –57 ppm [19], downfield to T₃) were detected. The range of ²⁹Si NMR chemical shift of T₃ units in silsesquioxanes depends on the geometry of the system and type of substituents at silicon atoms. For example, T₃ are more deshielded in strained six-membered triangular cycles and show their resonances in the region (–54) to (–55) ppm [2]. The chemical shift of T₃ unit moves upfield on decrease of the steric strain in siloxane ring [20]. ²⁹Si CP MAS spectra obtained for PT_{Si}SS (I-A, II-A, III-A, III-B, III-C and IV-A)

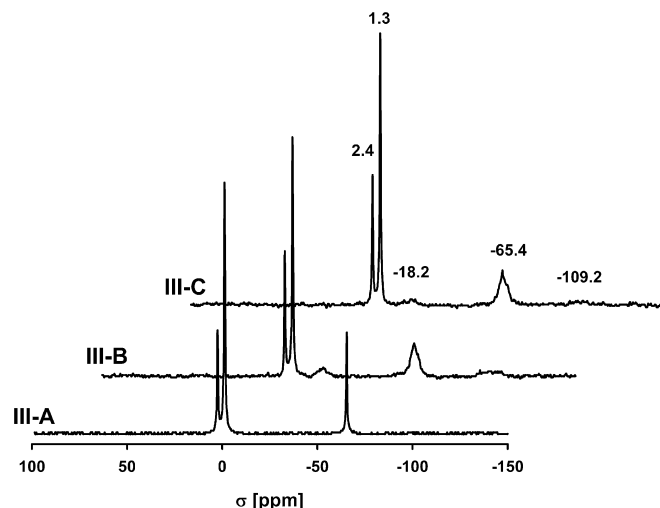


Fig. 3. ²⁹Si CP MAS NMR of PT_{Si}SS obtained in CH₂Cl₂ (samples III-A, III-B and III-C).

did not show any significant resonance between 40 ppm and 60 ppm. Consequently, all PT_{Si}SS are predominantly composed of eight-membered siloxane rings.

NMR spectroscopy can be also a powerful tool for confirmation of regularity of a silsesquioxane ladder. Typically, if a macromolecule demonstrates two Bragg peaks in its XRD pattern, and the resonance peak corresponding to the repeating T₃ units in its NMR spectrum has a narrow width at half peak (*W*_{1/2}), the macromolecule can be considered as a highly-ordered one (the narrower *W*_{1/2}, the higher the structure regularity). A substantial difference between *W*_{1/2} of T₃ peak at –65.3 ppm in crystalline sample III-A, and other fractions was observed. Peak of III-A is sharp (*W*_{1/2} = 0.8 ppm) and well defined (typical for a polyhedral POSS). It differs from the broad resonances (*W*_{1/2} ≈ 5 ppm) recorded for ladder-like polymeric PT_{Si}SS. As shown for other silsesquioxane systems with bulky substituents [21], resonance line broadening for ladder-like PT_{Si}SS can be attributed, beside stereochemical differences in the environment of T₃, to large steric hindrance of (Me₃Si)₃CSiMe₂–CH₂CH₂– group that results in reduced mobility of T₃ unit. Resonances corresponding to Me₃Si– (1.3 ppm) and –SiMe₂– (2.4 ppm) groups, which are situated in the exterior of the molecule, appear as sharp signals (*W*_{1/2} = 0.8 ppm for all the samples). ¹³C CP MAS NMR spectra (Fig. 4) show similar dependence.

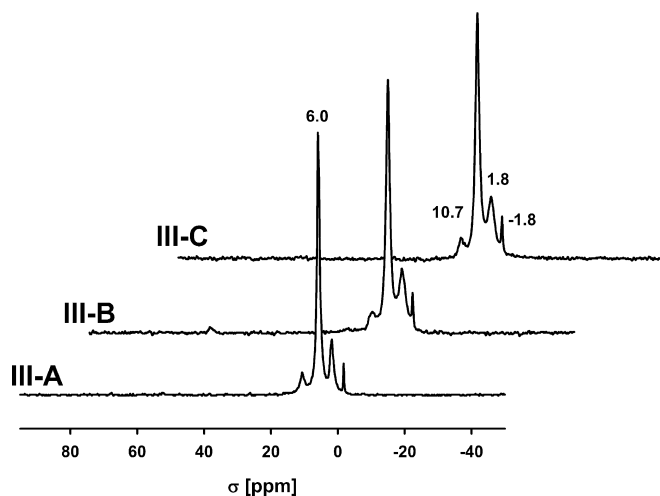


Fig. 4. ¹³C CP MAS NMR of PT_{Si}SS obtained in CH₂Cl₂ (samples III-A, III-B and III-C).

It proves that polymeric silsesquioxanes of postulated ladder-like structure are relatively ordered.

^{29}Si CPMAS NMR spectra of polymeric $\text{PT}_{\text{Si}}\text{SS}$ materials proved also the presence of D and Q-type units in the silsesquioxane framework, resulting from side reactions involving a nucleophilic attack of fluoride ion on $-\text{CH}_2-\text{SiO}_{3/2}$ silicon atom [14]. Silicon-carbon bond breaking as a result of nucleophilic activation was already reported in sol-gel reactions catalyzed by fluoride ions [22]. The concentration of Q units is not high and varies in $\text{PT}_{\text{Si}}\text{SS}$ fractions. The fraction I-B obtained in EtOH, seems to suffer most on this process. Its ^{29}Si MAS NMR spectrum (Fig. 5) indicated the presence of two Q type siloxane structures (-99.7 ppm and -109.1 ppm) in 2.2/2.9/1 respective ratio to T_3 at -65.3 ppm. ^{13}C MAS NMR spectrum of I-B, apart from the set of peaks typical to $\text{PT}_{\text{Si}}\text{SS}$, showed also resonances at 58.8 ppm and 19.5 ppm (identified as unreacted $-\text{SiOEt}$ groups) as well as two other at 24.1 ppm and 13.2 ppm (chemical shift range typical to methylene carbons). Elemental analysis has proved a substantial decrease of carbon and hydrogen content in I-B (Table 1). Thermogravimetric analysis has shown that the residue left after pyrolysis of I-B in N_2 is much bigger than those obtained for other $\text{PT}_{\text{Si}}\text{SS}$ (Fig. 6), which also suggests relatively high content of $-\text{SiOSi}-$ bonds in I-B. Si-F groups were not detected in all samples (^{19}F NMR).

2.2.3. FTIR characteristics

High degree of condensation of silanol groups in the obtained fractions of $\text{PT}_{\text{Si}}\text{SS}$ was confirmed by FTIR (Fig. 7). Bands related to stretching vibration of $-\text{SiOH}$ end groups (expected at ~ 930 cm^{-1} and ~ 3500 cm^{-1} [23]) were almost not observed (Fig. 7a). Also, only traces of $-\text{SiOEt}$ (950 cm^{-1}) were detected. All samples show similar characteristic vibrations [aliphatic C-H stretching bands in the 2900 cm^{-1} region, a sharp band of $\delta(\text{Si}-\text{CH}_3)$ mode at 1261 cm^{-1} and $\rho(\text{Si}-\text{CH}_3)$ at 856 cm^{-1}]. More discrete differences can be observed in 1200 – 900 cm^{-1} region (Fig. 7b). It is known that strainless caged and ring structures show a strong $\nu(\text{Si}-\text{O}-\text{Si})$ stretching absorption in 1115 – 1150 cm^{-1} frequency region [24]. A single $\nu(\text{Si}-\text{O}-\text{Si})$ band here may evidence the presence of polyhedral silsesquioxane structures of T_8 to T_{14} type [25]. Indeed, the crystalline sample III-A shows a narrow band centred at 1122 cm^{-1} . Ladder-like silsesquioxanes usually have two adsorption bands ($\nu_{\text{ring-sym}}$ at ~ 1040 cm^{-1} and $\nu_{\text{ring-asym}}$ at ~ 1130 cm^{-1}) in the discussed IR region [5e,16b,24f]. Higher frequency mode $\nu_{\text{ring-asym}}$ corresponds to parallel, and $\nu_{\text{ring-sym}}$ to anti-parallel displacements of oxygen atoms on opposite sides of a siloxane ring. Intensity of these stretching modes can be linked to symmetry of cyclic silsesquioxane structures [24f]. However, the position of $\nu(\text{Si}-\text{O}-\text{Si})$ modes can be obscure in particular cases. For example well-defined, highly regular ladder silsesquioxanes

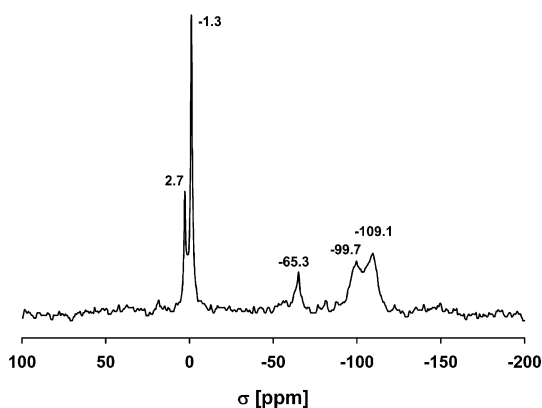


Fig. 5. ^{29}Si CPMAS NMR of resinous $\text{PT}_{\text{Si}}\text{SS}$ (I-B).

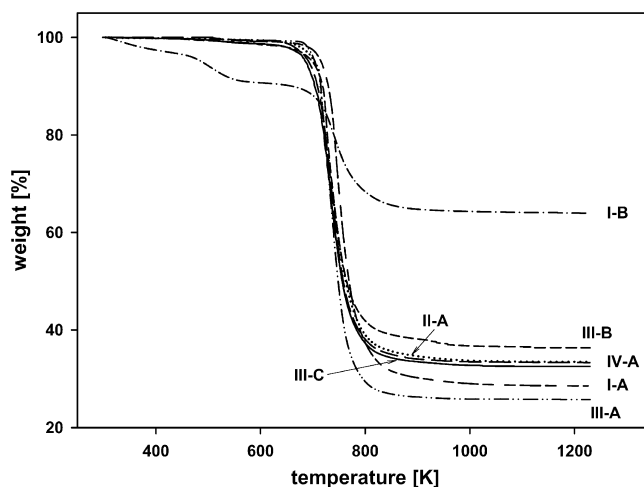


Fig. 6. Comparative thermal decomposition study (TGA) of $\text{PT}_{\text{Si}}\text{SS}$ in N_2 (10 K/min).

were reported to have one dominant $\nu(\text{Si}-\text{O}-\text{Si})$ band at 1045 cm^{-1} [16d] or 1026 cm^{-1} [5c]. A single IR band was observed at 1121 cm^{-1} for silsesquioxanes bearing bulky side substituents [21]. Samples of $\text{PT}_{\text{Si}}\text{SS}$ of postulated ladder-like structure have two broad and merging bands corresponding to $\nu(\text{Si}-\text{O}-\text{Si})$ adsorption – a dominant one at 1110 – 1122 cm^{-1} and an additional weak shoulder at 1063 cm^{-1} . $\nu(\text{Si}-\text{O}-\text{Si})$ band of sample II-A is asymmetric (its maximum is shifted towards $\nu_{\text{ring-asym}}$ mode) due to the presence of crystalline polyhedral species. IV-A of most regular ladder-like framework (as indicated by XRD data) among the studied samples, has also most defined 1122 cm^{-1} shoulder of $\nu(\text{Si}-\text{O}-\text{Si})$ band. The observation that for all the samples of polymeric $\text{PT}_{\text{Si}}\text{SS}$ asymmetric $\nu(\text{Si}-\text{O}-\text{Si})$ mode at ~ 1120 cm^{-1} predominates, is of particular interest. It can be assumed that ladder-like $\text{PT}_{\text{Si}}\text{SS}$ are build of silsesquioxane rings of geometry close to the one observed for polyhedral species. Similar Si-O-Si angles can be induced by the presence of hindered T_{Si} moieties.

2.2.4. Molecular mass measurements

Due to the reasonable solubility of $\text{PT}_{\text{Si}}\text{SS}$, their molecular masses could be studied using multiple detection SEC [RI, light scattering (MALLS and RALLS) and differential viscometer] (Table 1). We have found that some samples were contaminated by a small fraction of insoluble microgel (the presence of Q units can be the reason). The difference between the injected mass and the one calculated using $\delta n/\delta C$ (MALLS), can be expressed by the concentration index $[C_c]/[C_i]$ (Table 1). Well soluble samples of $\text{PT}_{\text{Si}}\text{SS}$ have their $[C_c]/[C_i] \geq 0.92$ (ideal value $[C_c]/[C_i] = 1.0$). Molecular masses of the soluble fractions were found to be rather low. Using both light scattering methods, MALLS and RALLS, masses of ~ 3500 D were obtained. They correspond to the one calculated for $\text{PT}_{\text{Si}}\text{SS}$ with an average degree of polycondensation $n = 10$. Values obtained by MALLS and RALLS are similar, except for III-B, which showed also a bimodal distribution of molecules. SEC traces recorded for other samples are quite sharp and symmetrical. Low values of M_n (1300 – 1600 D) obtained with RI method, small intrinsic viscosity $[\eta]$ (0.0205 – 0.0281 dL/g) and hydrodynamic radius R_h (1.05 – 1.24 nm) of the studied samples suggest that the soluble polymeric chains have compact structure in solution.

MALDI analysis was carried out for all the obtained products, and it was found that the range of recorded m/z corresponds to values obtained using MALLS and RALLS. In spite of the described above, reliable analytic results (NMR, FTIR) pointing to high degree of conversion of $-\text{SiOEt}$ and $-\text{SiOH}$ groups, completely condensed species (for example polyhedral T_8 , T_{10} or T_{12} $\text{PT}_{\text{Si}}\text{SS}$) did not give an appropriate response in MALDI. Instead, incompletely con-

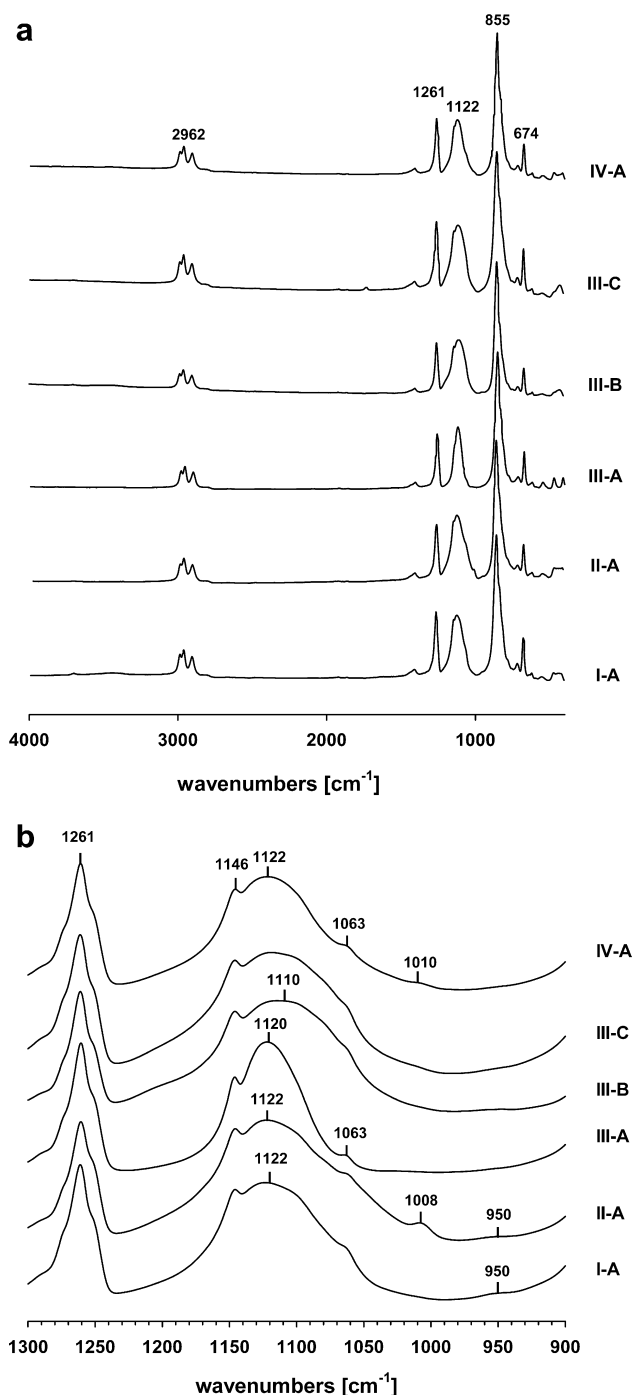


Fig. 7. FTIR spectra of $PT_{Si}SS$ (a) – complete spectra, (b) extension of Si–O–Si region.

densified molecules of polyhedral framework (T_7 , T_8 and T_9) were detected as preponderant (Fig. 8). However, ^{29}Si NMR and FTIR analysis proved that the samples indeed contain very few –SiOEt or –SiOH functionalized species. Moreover, judging by XRD, NMR and FTIR measurements, the main part of all studied $PT_{Si}SS$ samples (except III-A) has in fact ladder-like structure. Unsatisfactory MALDI results can be thus explained in terms of a very difficult ionization of nonpolar, highly condensed $PT_{Si}SS$.

2.3. Specific properties of hybrid carbosilane–silsesquioxane materials

Silsesquioxanes of a defined structure are often used for preparation of new multifunctional materials (polymer nanocomposites

and hybrids) having increased thermal resistance and good mechanical properties [26]. The mechanism of thermal degradation of a POSS material depends on the structure of silsesquioxane unit (cage, ladder-like or random network) and the type of organic group R on Si atom [27]. When heated in an inert atmosphere, polyhedral silsesquioxanes with small substituents undergo sublimation (430–530 K range for $R = H, Me, Vi$) or evaporation after melting (580–630 K for $R = i-Bu$ or octyl). Increasing the alkyl chain length (from C_2 to C_{10}) a substantial shift of the weight loss onset to higher temperatures was observed [28]. On the other hand, phenyl functionalized octahedral silsesquioxane shows higher thermal stability (up to 620 K) and low volatility [27]. Polymeric silsesquioxanes can be generally processed to higher temperatures than their polyhedral counterparts (for example, polymeric vinylsilsesquioxane is stable up to ~ 720 K [27]) and their decomposition at high temperatures can be yet impeded. For instance, thermal stability of a ladder-like poly(vinylsilsesquioxane) was increased by vinyl groups polymerization. As a consequence 5% mass loss was observed only at ~ 900 K [29]. Incorporation of fluorine-containing side chains to ladder-like poly(epoxysilsesquioxanes) also delayed their thermal decomposition, both in nitrogen and air (5% weight loss was observed at 700 K) [30]. Quite often, for ladder-like silsesquioxanes, thermal decomposition occurs in the vitreous state (below glass transition) because of the steric hindrance provided by side substituents at each repeating unit, and consequently, a retardation of segmental motion of polymer chains [31].

Poly(silsesquioxanes), due to their mixed cage/network structure, thermal stability and mechanical hardness, have been recognized as potential candidates for low dielectric constant materials [32]. The use of low- κ dielectric materials of silsesquioxane structure [with dielectric constants lower than 3.9, which is the value characteristic of SiO_2] receive growing attention for components separation in microelectronic devices [33]. Periodic mesoporous organosilica thin films derived from bridged alkoxy silanes and tetramethylorthosilicate can be used as low- κ layers in microelectronics [34]. They are hydrophobic, thermally and mechanically stable, and have low dielectric constant (decreasing to values as low as 1.8 with the increase of the organic content). [Cyclohexenylethyl $Me_2SiOSiO_{1.5}$] $_4$ –[H $Me_2SiOSiO_{1.5}$] $_4$, cross-linked by means of thermal hydrosilylation can be another example of a good dielectric hybrid material [10d]. The precursor melts at 350 K and can be easily cast and cured to leave a cross-linked product, which is stable in air above 670 K and shows good dielectric properties ($\kappa = 2.8$ –2.9). The value of κ of a hybrid silsesquioxane material can be also lowered by the replacement of Si–O bonds with less polarizable Si–C bonds (which also results in lowered both material shrinkage and H_2O uptake [35]), or breaking up Si–O–Si network by large organic moieties (porosity generation). For example, the use of large adamantylphenol substituents gave POSS materials of dielectric constant $\kappa = 1.9$ –2.3 [36]. Tethering covalently polyhedral POSS to organic polymers can also give organic–inorganic nanocomposite materials with low dielectric constant ($\kappa \approx 2.3$) and good mechanical properties [37].

2.3.1. Thermal analysis of $PT_{Si}SS$

$PT_{Si}SS$ were found to be hydrophobic and extremely thermally resistant. Five percent weight loss was observed only at about 700 K during the thermogravimetric analysis carried out in nitrogen (Fig. 6). Thermolysis of $PT_{Si}SS$ occurred sharply at ~ 720 K. No sublimation on heating was observed, and a substantial char residue ($\sim 30\%$) was left at 1100 K. All $PT_{Si}SS$ were analyzed by DSC method and showed typically a particular thermal transition at 313 K (Fig. 9, melting was not observed in the studied temperature range of 220–570 K). Usually, in a DSC trace of a regular amorphous polymeric system, such a steep slope indicates glass

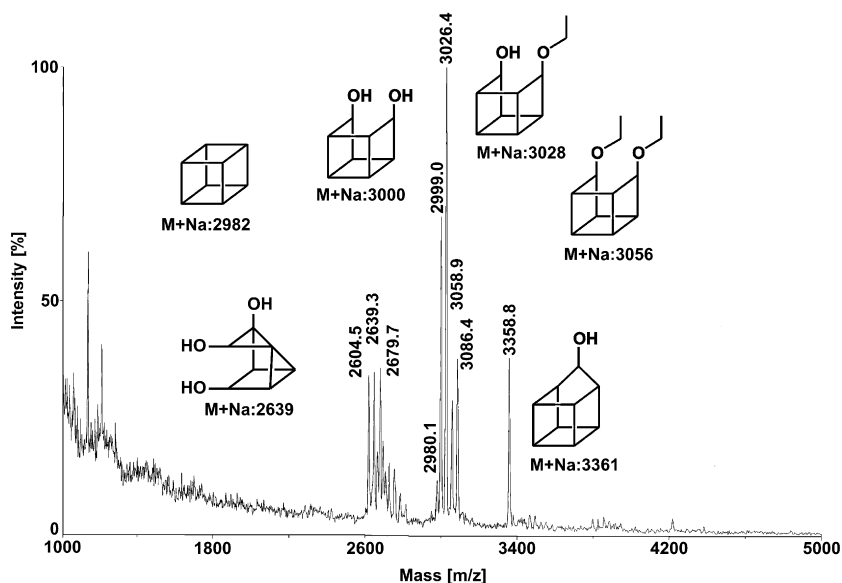


Fig. 8. MALDI of I-A – $(\text{Me}_3\text{Si})_3\text{CSiMe}_2\text{CH}_2\text{CH}_2-$ substituents were omitted for clarity of the presented structures.

transition (T_g), involving heat capacity change as the polymer matrix transforms from the glassy state to the rubbery state. Ladder polysilsesquioxanes usually show T_g at higher temperatures than those observed for corresponding single-chain siloxanes. For rigid $\text{PT}_{\text{Si}}\text{SS}$ molecules the transition at 313 K is not a glass transition involving segmental movements of the double siloxane chain. Due to an enormous anchoring effect provided by sterically hindered T_{Si} moiety, a single-chain linear siloxane having $(\text{Me}_3\text{Si})_3\text{CSiMe}_2\text{CH}_2\text{CH}_2-$ groups at each silicon atom did not show any T_g before its thermal decomposition [8h]. Thus, judging by the effect exerted by T_{Si} groups on linear analogues, double-chain $(\text{Me}_3\text{Si})_3\text{CSiMe}_2\text{CH}_2\text{CH}_2-$ substituted ladder-like silsesquioxanes should rather decompose before their devitrification. ^{29}Si CPMAS NMR studies of $\text{PT}_{\text{Si}}\text{SS}$ at variable temperatures indicated a decrease of intensity of the resonance corresponding to $(\text{Me}_3\text{Si})_3\text{C}$ -unit above 313 K (without peak broadening) (Fig. 9). The resonances of $-\text{SiMe}_2-$ and $-\text{CH}_2\text{SiO}_3-$ groups were found to be insensitive to the change of temperature. The same trend was observed by ^{13}C CPMAS NMR (Fig. 10). The transition at 313 K is thus assumed to be related to a selective decrease of the relaxation

time, which in a NMR experiment is usually observed for fast rotating groups. The observed phenomena seem to prove that the thermal transition can be related to an increase of mobility of Me_3Si groups. These findings can be of importance also concerning the mechanism of thermal decomposition of $\text{PT}_{\text{Si}}\text{SS}$ [38]. It was shown before, that selective decomposition of $\text{C}-\text{SiMe}_3$ bonds occurred on exposition of polysiloxanes, modified with side $(\text{Me}_3\text{Si})_3\text{C}(\text{CH}_2)_5-$ groups, to UV-laser light [8e]. Thus, thermal degradation of $\text{PT}_{\text{Si}}\text{SS}$ occurring at 720 K can be probably related to $\text{C}-\text{SiMe}_3$ bond breaking.

2.3.2. Dielectric constant measurements

$\text{PT}_{\text{Si}}\text{SS}$ materials combine all the trends that can be beneficial for lowering dielectric constant. T_{Si} group is large, composed of nonpolar $\text{Si}-\text{C}$ bonds. Its steric requirements allow not only for the formation of silsesquioxanes of regular structure, with siloxane clusters separated by carbosilane matrix, but also for an increase of free volume in the material. Preliminary tests indicated that the aver-

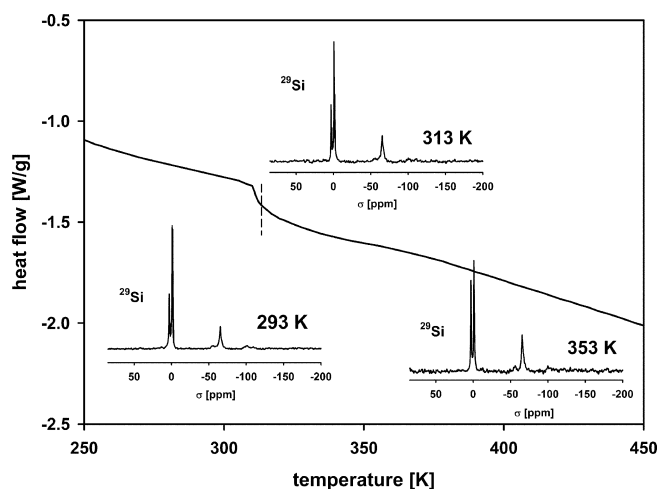


Fig. 9. DSC thermogram of I-A and its ^{29}Si CPMAS NMR spectra corresponding to specific temperatures.

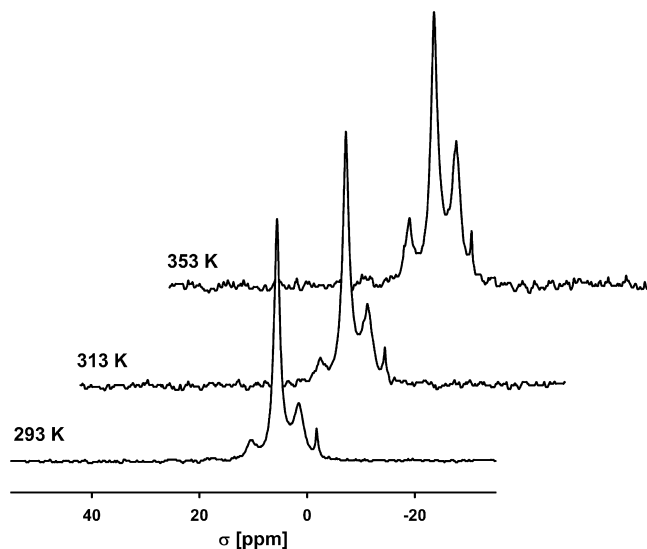


Fig. 10. ^{13}C CPMAS NMR spectra of I-A recorded at specific temperatures.

age dielectric constant κ of the obtained $PT_{Si}SS$ materials is ≤ 1.9 F/m. For the measurements, samples of $PT_{Si}SS$ (II-A, III-B, III-C) were pressed into continuous, uniform pieces. Unfortunately, they were not resistant enough (polyhedral $PT_{Si}SS$ III-A could not be pressed into tablets) and any mechanical tests could not be performed. The current works are focused on κ measurements in thin films of $PT_{Si}SS$, as well as formation of monolithic $PT_{Si}SS$.

3. Conclusions

A new class of hybrid materials – carbosilane–silsesquioxanes ($PT_{Si}SS$) – was synthesized. They were prepared in the hydrolytic condensation process catalyzed by a nucleophilic catalyst (TBAF) and using a novel precursor $[(Me_3Si)_3CSiMe_2CH_2CH_2Si(OEt)_3]$ which combines extremely sterically demanding tris(trimethylsilyl)methyl unit and alkoxy-silyl function. The reaction conditions were found to govern the structure of products. Aprotic solvents of low polarity promote formation of crystalline species. However, the fraction of these polyhedral moieties is relatively small. The main part of the product has an ordered, ladder-like structure generated due to the specific steric requirements of nonpolar $(Me_3Si)_3CSiMe_2CH_2CH_2-$ groups (a “self-template” effect). Formation of a ladder-like siloxane framework is independent on the type of solvent. Nevertheless, the higher polarity of the reaction medium, the lower degree of order and more frequent side reactions occurring at T_3 silicone atom due to nucleophilic attack of fluoride ions. All $PT_{Si}SS$ are solids of a high level of condensation, reasonably soluble in common organic solvents and thermally stable (in nitrogen) up to ~ 720 K. Average dielectric constant κ measured for selected $PT_{Si}SS$ samples was found to be ~ 1.9 F/m.

4. Experimental part

4.1. Analysis and general methodology

Liquid state NMR spectra of precursors and condensed soluble materials were recorded in $CDCl_3$ as a solvent on DRX-500 MHz (1H , ^{13}C and ^{29}Si NMR) spectrometer with TMS as the reference. Solid state NMR spectra were recorded on a Bruker MSL-300 MHz spectrometer (59.6 MHz for ^{29}Si and 75.5 MHz for ^{13}C) using a Bruker CP MAS probe with a 4 mm zirconium rotor. The peak positions were referenced to the signal of Q_8M_8 (trimethylsilyl ester of cubic octameric silicate) standard. 1H - ^{29}Si CP MAS and 1H - ^{13}C CP MAS NMR experiments were performed with sample spinning rates of 6 kHz and 8 kHz, respectively. Contact times (t) were 3 ms for ^{29}Si and 2.5 ms for ^{13}C with recycling delay of 6 s. Gaussian apodization was used to increase signal to noise ratio, which resulted in broadening of resonance lines of less than 1 ppm. GC-MS CI+ analysis was carried out with a Finnigan MAT 95 spectrometer at 70 eV.

FTIR spectra were recorded with a Bio-Rad FTS-60 spectrometer. Spectra were collected in the mid and far infrared regions (4000 – 100 cm^{-1}) after 256 scans at 2 cm^{-1} resolution. Samples were prepared by the standard KBr and polyethylene (Merck) pellets methods. Spectra of soluble precursors $[(Me_3Si)_3CSiMe_2CH=CH_2]$ and $(Me_3Si)_3CSiMe_2CH_2CH_2Si(OEt)_3]$ were recorded as thin films on a KBr plate.

Differential Scanning Calorimetry traces were recorded with a 2920 Modulated DSC apparatus (TA Instruments) calibrated against indium and copper in nitrogen atmosphere at the temperature range: 220 – 570 K (first and second heating). Thermograms were taken for samples about 10 mg, placed in hermetic aluminum pans, and heated/cooled at 10 K/min. Each thermal treatment was repeated two times for each sample. The transition temperatures were taken from the second run.

Thermogravimetric analyses were performed by the use of a Hi-Res TGA 2950 Thermogravimetric Analyzer (TA Instruments) in nitrogen or air atmosphere (heating rate 10 K/min, resolution 3 , sensitivity 3).

Scanning electron microscopy was performed using SEM Scanning Electron Microscope JSM-5500 LV (Jeol) apparatus with samples attached to brass supports using an adhesive tape, and their surface was sputter-coated with gold.

The crystalline structure was detected by wide-angle X-ray powder diffraction measurement (WAXS) performed using Philips X'Pert Pro MD diffractometer. Radiation used was Cu $K\alpha_1$ line monochromatized by $Ge(111)$ monochromator. Standard Bragg-Brentano geometry with θ - 2θ setup was applied (0.008° step size and 5 – 90° 2θ range).

Size exclusion chromatography (SEC) was performed as described before [39], using a Wyatt Optilab 903 apparatus [LKB 2150 HPLC pumps, dual detector MALLS (Multiangle Laser Light Scattering)/RI, two (TSK G4000HLX and G2000HLX) columns] and Viscotek 270 dual detector [right angle laser light scattering, at $\lambda = 670$ nm (RALLS) and differential viscometer]. CH_2Cl_2 was used as the eluent (0.8 ml/min). Samples were immersed in CH_2Cl_2 , left overnight (concentration of polymers: 1 mg/ml) and filtered through 0.2 μm pore size SRP membrane filters.

MALDI TOF spectra of the samples were recorded with Voyager-Elite mass spectrometer. NaI was used as the cationizing agent, and ditranol as the matrix.

Dielectric constant measurements were obtained using a Hewlett-Packard 4284A precision LCR meter at 1 kHz. Specimens were prepared as a pressed, transparent tablets (1.4 cm of diameter, 400 μm thick) using 1 ton hydraulic press after the evacuation of the chamber to 0.1 kPa. The height of specimens was measured directly with a micrometer. The sample was set between two aluminum plates with attached copper electrodes to measure the dielectric constant at the selected frequency.

4.1.1. Reagents

Trimethylchlorosilane (98 %), bromoform (96 %), $nBuLi$ (2.5 M solution in hexanes), $MeLi$ (1.6 M solution in diethyl ether) as well as tetrabutylammonium fluoride [TBAF, 1 M solution in THF (contains 5% of water)] were purchased from Aldrich. Platinum divinyltetramethyldisiloxane complex (Karstedt's catalyst, 3% solution in xylenes), chlorodimethylvinylsilane (97%) and triethoxysilane (97%) were bought from ABCR. Tris(trimethylsilyl)methane $HC(SiMe_3)_3$ [40] was prepared according to the respective literature procedures. Solvents (tetrahydrofuran, diethyl ether, pentane, methylene chloride, ethyl alcohol, acetone) were supplied by POCh (Polish Chemical Reagents). All solvents were carefully dried according to the literature procedures [41] and distilled prior to their use. Other reagents were used as received. All syntheses were performed using standard Schlenk or syringe techniques under an atmosphere of argon.

4.2. Synthetic procedures

4.2.1. Synthesis of tris(trimethylsilyl)(vinyl)dimethylsilyl)methane

Fifteen milliliters of $MeLi$ in diethyl ether (1.6 M solution, 0.024 mol) was placed in a Schlenk's flask. Volatiles were removed under vacuum and a solution of $HC(SiMe_3)_3$ (5.06 g, 0.022 mol) in THF (30 ml) was added. The solution became yellowish after 10 min of stirring at room temperature. It was stirred at 343 K for additional 2 h and then cooled to room temperature. $ClSiMe_2CH=CH_2$ (3.6 ml, 0.026 mol) was added drop-wise at room temperature to the prepared solution $LiC(SiMe_3)_3/THF$. The mixture became colourless gradually, on chlorosilane addition. It was then stirred for additional 24 h at 343 K. Volatiles were removed under reduced pressure, and the product was dissolved in diethyl ether

(100 ml). The solution was washed with cold water to neutral pH and dried over MgSO_4 , then separated. The crude product, after volatiles removal on a Rotary evaporator, was dried (for 16 h under vacuum at room temperature) to leave a solid material. Pure $(\text{Me}_3\text{Si})_3\text{CSiMe}_2\text{CH}=\text{CH}_2$ (6.05 g, $Y = 87\%$) was isolated by sublimation at 353 K/1 Pa.



$^1\text{H NMR}$ (σ ppm): 0.26 (s) SiMe_3 (27H), 0.32 (s) SiMe_2 (6H), 5.65 (m) $=\text{CH}_2$ (1H), 5.91 (m) $=\text{CH}_2$ (1H), 6.35 (m) $-\text{CH}=(1\text{H})$.

$^{13}\text{C NMR}$ (σ ppm): 3.1 SiMe_2 , 5.3 SiMe_3 , 130.3 $=\text{CH}_2$, 143.2 $-\text{CH}=\text{}$.

$^{29}\text{Si NMR}$ (σ ppm): -8.3 SiMe_2 , -1.0 SiMe_3 .

MS-Cl (m/z): 301 ($\text{M}-\text{Me}$) $^+$ 100%, 213 ($\text{M}-\text{SiMe}_4-\text{Me}$) $^+$ 16%, 201 ($\text{M}-\text{SiMe}_4-\text{Vi}$) $^+$ 6%, 73 (SiMe_3) $^+$ 50%.

Elemental Anal. Calc.: C, 53.08; H, 11.45. Found: C, 52.71; H, 11.63%.

FTIR: 2974.3, 2900.8, 1390.4, 1259.0, 1168.3, 1142.9, 1106.2, 1081.8, 861.7, 847.5, 814.9, 783.3, 673.3.

4.2.2. Synthesis of tris(trimethylsilyl)[(1-triethoxysilyl)ethyl]dimethylsilyl]methane

A solution of $(\text{Me}_3\text{Si})_3\text{CSiMe}_2\text{CH}=\text{CH}_2$ (1.02 g, 0.0032 mol) and triethoxysilane (0.88 g, 0.0054 mol) ($[\text{SiH}]/[\text{CH}_2=\text{CH}-] = 1.7$) in toluene (20 ml) was prepared. Platinum catalyst ($[\text{Pt}]/[\text{CH}_2=\text{CH}-] = 5 \times 10^{-4}$) was added to the reaction mixture and the reaction was carried out at room temperature. The composition of the reaction mixture was studied by FTIR. After 48 h, once the addition to $\text{CH}_2=\text{CH}-$ was completed, the volatiles were removed under reduced pressure to leave $(\text{Me}_3\text{Si})_3\text{CSiMe}_2\text{CH}_2\text{CH}_2\text{Si}(\text{OEt})_3$ with quantitative yield. The product (viscous, colourless oil) was analyzed and used without purification for the synthesis of silsesquioxane materials.



$^1\text{H NMR}$ (σ ppm): 0.20 (s) SiMe_2 (6H), 0.23 (s) SiMe_3 (27H), 0.5 (m) CH_2 (2H), 0.8 (m) CH_2 (2H), 1.22 (t) OCH_2CH_3 , 3.79 (q) OCH_2CH_3 .

$^{13}\text{C NMR}$ (σ ppm): -1.8 C_q , 0.9 SiMe_2 , 2.9 CH_2 , 5.3 SiMe_3 , 10.1 CH_2 , 18.1 OCH_2CH_3 , 57.9 OCH_2CH_3 .

$^{29}\text{Si NMR}$ (σ ppm): 2.0 SiMe_2 , -2.0 SiMe_3 , $-45.7 \text{ Si}(\text{OEt})_3$.

MS-Cl: 481 ($\text{M}+1$) $^+$ 40%, 465 ($\text{M}-\text{Me}$) $^+$ 100%, 421 6%, 289 23%, 73 (SiMe_3) $^+$ 3%.

Elemental Anal. Calc.: C, 49.94; H, 10.90. Found: C, 49.85; H, 10.53%.

FTIR: 2983.3, 2957.8, 2903.0, 1400.4, 1257.9, 948.5, 852.7, 784.3, 671.9.

4.2.3. Preparation of silsesquioxane materials by TBAF-catalyzed hydrolytic condensation of tris(trimethylsilyl)[(1-triethoxysilyl)ethyl]dimethylsilyl]methane – a general procedure

$(\text{Me}_3\text{Si})_3\text{CSiMe}_2\text{CH}_2\text{CH}_2\text{Si}(\text{OEt})_3$ (1.54 g, 0.0032 mol) was diluted with a given solvent, to obtain the concentration $[\text{SiO}-\text{Et}] = 0.49 \text{ mol/dm}^3$. To the solution (stirred at room temperature), TBAF solution in THF was added with a syringe in one run ($[\text{SiO}-\text{Et}]/[\text{F}] = 4.9$, $[\text{SiOEt}]/[\text{H}_2\text{O}] = 6.6$). The stirring was continued at room temperature for 72 h, and the mixture got turbid after a certain time. It was then filtered and the precipitate (white solid labeled fraction A for each experiment) was washed with large volumes of EtOH, toluene and acetone, and then dried under high vacuum to constant weight. The filtrate was concentrated and then dissolved in CH_2Cl_2 and precipitated into a large volume of EtOH. The second solid precipitate (fraction B) was also separated and dried under high vacuum. In the experiment carried out in CH_2Cl_2 the filtrate was composed of soluble fine particles (that precipitated on concentration of the filtrate) and completely soluble polymeric material. The latter was precipitated into EtOH to give fibrous particles. The fractionated products were analyzed by ^1H

NMR, ^{13}C and ^{29}Si CP MAS NMR, TGA, FTIR and SEM (see the results discussion).



$^1\text{H NMR}$ (σ ppm): 0.19 (s) SiMe_2 (6H), 0.23 (s) SiMe_3 (27H), 0.45 (m) CH_2 (2H), 0.8 (m) CH_2 (2H).

$^{13}\text{C NMR}$ (σ ppm, in CDCl_3): -1.6 C_q , 1.5 SiMe_2 , 3.5 CH_2 , 5.6 SiMe_3 , 10.6 CH_2 .

$^{13}\text{C CP MAS NMR}$ (σ ppm): -1.8 C_q , 1.7 ($\text{SiMe}_2 + \text{CH}_2$) 5.7 SiMe_3 , 10.6 CH_2 .

$^{29}\text{Si CP MAS NMR}$ (σ ppm): 2.7 SiMe_2 , -1.4 SiMe_3 , $-65.4 \text{ SiO}_{3/2}$.

FTIR: 2986, 2962, 2905, 1408, 1261, 1146, 1122, 855, 717, 674.

Acknowledgements

The joint financial support by Centre of Molecular and Macromolecular Studies (Polish Academy of Sciences) and Polish Ministry of Science and Higher Education (Grant No. R05 0005 04 for NR 05-0005-04) is kindly acknowledged. We thank our colleagues for their kind help and comments [dielectric constant measurements of $\text{PT}_{\text{Si}}\text{SS}$ – Prof. Jeremiasz Jeszka and Mgr. Łukasz Pietrzak (CMMS, PAS), FTIR – Dr. hab. Włodzimierz Mozgawa (AGH)].

NMR was carried out in Laboratory for Analysis of Organic Compounds and Polymers, TGA and DSC analyses were done at Laboratory of Microanalysis and SEC was carried out in Department of Polymer Chemistry (CMMS, PAS). FTIR spectra were measured at Faculty of Materials Science and Ceramics (AGH).

References

- [1] R.H. Baney, M. Itoh, A. Sakakibara, T. Suzuki, Chem. Rev. 95 (1995) 1409–1430.
- [2] M. Unno, S.B. Alias, H. Sato, H. Matsumoto, Organometallics 15 (1996) 2413–2414.
- [3] (a) H.-J. Kim, J.-K. Lee, J.-B. Kim, E. S. Park, S.-J. Park, D.Y. Yoo, D.Y. Yoon, J. Am. Chem. Soc. 123 (2001) 12121–12122; (b) A.R. Bassindale, Z. Liu, I.A. MacKinnon, P.G. Taylor, Y. Yang, M.E. Light, P.N. Horton, M.B. Hursthouse, J. Chem. Soc., Dalton Trans. (2003) 2945–2949.
- [4] (a) G. Cerveau, R.J.P. Corriu, E. Framery, J. Mater. Chem. 10 (2000) 1617–1622; (b) G. Cerveau, R.J.P. Corriu, E. Framery, J. Mater. Chem. 11 (2001) 713–717; (c) G. Cerveau, R.J.P. Corriu, E. Framery, S. Ghosh, H.P. Mutin, J. Mater. Chem. 12 (2002) 3021–3026.
- [5] (a) H. Tang, J. Sun, J. Jang, X. Zhou, T. Hu, P. Xie, R. Zhang, J. Am. Chem. Soc. 124 (2002) 10482–10488; (b) J.J.E. Moreau, L. Vellutini, M. Wong Chi Man, C. Bied, Ph. Dieudonné, J.-L. Bantignies, J.-L. Sauvajol, Chem. Eur. J. 11 (2005) 1527–1537; (c) K. Deng, T. Zhang, X. Zhang, A. Zhang, P. Xie, R. Zhang, Macromol. Chem. Phys. 207 (2006) 404–411; (d) T. Zhang, K. Deng, P. Zhang, P. Xie, R. Zhang, Chem. Eur. J. 12 (2006) 3630–3635; (e) M. Unno, T. Matsumoto, H. Matsumoto, J. Organomet. Chem. 692 (2007) 307–312.
- [6] (a) Y. Lu, H. Fan, N. Doke, D.A. Loy, R.A. Assink, D.A. LaVan, C.J. Brinker, J. Am. Chem. Soc. 122 (2000) 5258–5261; (b) A. Stein, B.T. Melde, R.C. Schroden, Adv. Mater. 12 (2000) 1403–1419.
- [7] (a) C. Eaborn, J.D. Smith, J. Chem. Soc., Dalton Trans. (2001) 1541–1552; (b) C. Eaborn, J. Chem. Soc., Dalton Trans. (2001) 3397–3406.
- [8] (a) A. Kowalewska, W.A. Stańczyk, S. Boileau, L. Lestel, J.D. Smith, Polymer 40 (1999) 813–818; (b) A. Kowalewska, W.A. Stańczyk, Chem. Mater. 15 (2003) 2991–2997; (c) A. Kowalewska, W.A. Stańczyk, in: N. Auner (Ed.), Organosilicon Chemistry VI. From Molecules to Materials, vol. 2, Wiley-VCH, Weinheim, 2005, pp. 729–733; (d) A. Kowalewska, W.A. Stańczyk, ARKIVOC v (2006) 110–115; (e) A. Kowalewska, J. Kupcik, J. Pola, W.A. Stańczyk, Polymer 49 (2008) 857–866; (f) A. Kowalewska, J. Organomet. Chem. 693 (2008) 2193–2199; (g) A. Kowalewska, B. Delczyk, in: F. Ganachaud, S. Boileau, B. Boury (Eds.), Silicon Based Polymers, Advances in Synthesis and Supramolecular Organization, Springer-Verlag, London, 2008, pp. 99–118 (Chapter 1(8)); (h) A. Kowalewska, B. Delczyk, J. Chruściel, e-Polymers (2009), in press.
- [9] (a) M.Z. Asuncion, I. Hasegawa, J.W. Kampf, R.M. Laine, J. Mater. Chem. 15 (2005) 2114–2121; (b) R.M. Laine, J. Mater. Chem. 15 (2005) 3725–3744.
- [10] (a) Ch. Zhang, F. Babonneau, Ch. Bonhomme, R.M. Laine, Ch.L. Soles, H.A. Hristov, A.F. Yee, J. Am. Chem. Soc. 120 (1998) 8380–8391; (b) R.M. Laine, Ch. Zhang, A. Sellinger, L. Viculis, Appl. Organometal. Chem. 12 (1998) 715–723;

- (c) K. Pielichowski, J. Njuguna, B. Janowski, J. Pielichowski, *Adv. Polym. Sci.* 201 (2006) 225–296;
(d) N. Takamura, L. Viculis, Ch. Zhang, R.M. Laine, *Polym. Int.* 56 (2007) 1378–1391.
- [11] E. Muller, F.T. Edelmann, *Main Group Met. Chem.* 22 (1999) 485–488.
[12] D.A. Loy, B.M. Baugher, C.R. Baugher, D.A. Schneider, K. Rahimian, *Chem. Mater.* 12 (2000) 3624–3632.
[13] A.R. Bassindale, H. Chen, Z. Liu, I.A. MacKinnon, D.J. Parker, P.G. Taylor, Y. Yang, M.E. Light, P.N. Horton, M.B. Hursthouse, *J. Organomet. Chem.* 689 (2004) 3287–3300.
[14] A. Kowalewska, K. Różga-Wijas, M. Handke, *e-Polymers* 10 (2008) 150.
[15] (a) G. Cerveau, R.J.P. Corriu, C. Fischmeister-Lepeytre, *J. Mater. Chem.* 9 (1999) 1149–1154;
(b) G. Cerveau, R.J.P. Corriu, E. Framery, *Polyhedron* 19 (2000) 307–313;
(c) G. Cerveau, R.J.P. Corriu, E. Framery, *Chem. Mater.* 13 (2001) 3373–3388.
[16] (a) J.F. Brown, L.H. Vogt, A. Katchman, J.W. Eustache, K.M. Kiser, *J. Am. Chem. Soc.* 82 (1960) 6194–6195;
(b) Ch. Liu, Y. Liu, Z. Shen, P. Xie, R. Zhang, J. Yang, F. Bai, *Macromol. Chem. Phys.* 202 (2001) 1581–1585;
(c) X. Zhang, P. Xie, Z. Shen, J. Jiang, Ch. Zhu, H. Li, T. Zhang, Ch.C. Han, L. Wan, S. Yan, R. Zhang, *Angew. Chem., Int. Ed.* 45 (2006) 3112–3116;
(d) Z.-X. Zhang, J. Hao, P. Xie, X. Zhang, Ch.C. Han, R. Zhang, *Chem. Mater.* 20 (2008) 1322–1330.
[17] A. González-Campo, B. Boury, F. Teixidor, R. Núñez, *Chem. Mater.* 18 (2006) 4344–4353.
[18] L.A.S. De A. Prado, E. Radavanovic, H.O. Pastore, I.V.P. Yoshida, I.L. Torriani, *J. Polym. Sci. Part A* 38 (2000) 1580–1589.
[19] A. Kowalewska, *J. Mater. Chem.* 15 (2005) 4997–5006.
[20] E. Rikowski, H.C. Marsmann, *Polyhedron* 16 (1997) 3357–3361.
[21] D.P. Fasce, R.J.J. Williams, F. Méchin, J.P. Pascault, M.F. Llauro, R. Pétiaud, *Macromolecules* 32 (1999) 4757–4763.
[22] (a) A. Adima, C. Bied, J.J.E. Moreau, M. Wong Chi Man, *Eur. J. Org. Chem.* (2004) 2582–2588;
(b) L.F. Campo, F.S. Rodembusch, F. Lerouge, J. Alauzun, G. Cerveau, R.J.P. Corriu, *C.R. Chim.* 11 (2008) 1271–1276.
[23] (a) C.Y. Wang, Z.X. Shen, J.Z. Zheng, *Appl. Spectrosc.* 54 (2000) 209–213;
(b) C.Y. Wang, Z.X. Shen, J.Z. Zheng, *Appl. Spectrosc.* 55 (2001) 1347–1351.
[24] (a) L.H. Vogt, J.F. Brown Jr, *Inorg. Chem.* 2 (1963) 189–192;
(b) Ch.Ch. Yang, W.Ch. Chen, *J. Mater. Chem.* 12 (2002) 1138–1141;
(c) Q.R. Huang, W. Volksen, E. Huang, M. Toney, C.W. Frank, R.D. Miller, *Chem. Mater.* 14 (2002) 3676–3685;
(d) Y. Jun, P. Nagpal, D.J. Norris, *Adv. Mater.* 20 (2008) 606–610;
(e) B. Handke, W. Jastrzębski, W. Mozgawa, A. Kowalewska, *J. Molec. Struct.* 887 (2008) 159–164;
(f) E.S. Park, H.W. Ro, C.V. Nguyen, R.L. Jaffe, D.Y. Yoon, *Chem. Mater.* 20 (2008) 1548–1554.
- [25] J.F. Brown, L.H. Vogt, P.I. Prescott, *J. Am. Chem. Soc.* 86 (1964) 1120–1125.
[26] C. Sanchez, G.J.A.A. Soler-Illia, F. Ribot, T. Lalot, C.R. Mayer, V. Cabuil, *Chem. Mater.* 13 (2001) 3061–3083.
[27] A. Fina, D. Tabuani, F. Carniato, A. Frache, E. Boccaleri, G. Camino, *Thermochimica Acta* 440 (2006) 36–42.
[28] C. Bolln, A. Tsuchida, H. Frey, R. Mülhaupt, *Chem. Mater.* 9 (1997) 1475–1479.
[29] L. Liu, Y. Hu, X. Li, Z. Chen, W. Fan, *Thermochim. Acta* 438 (2005) 164–171.
[30] J. Wang, Ch. He, Y. Lin, T.S. Chung, *Thermochim. Acta* 381 (2002) 83–92.
[31] J.D. Lichtenhan, Y.A. Otonari, M.J. Carr, *Macromolecules* 28 (1995) 8435–8437.
[32] (a) J.L. Hedrick, R.D. Miller, C.J. Hawker, K.R. Carter, W. Volksen, D.Y. Yoon, M. Trollsas, *Adv. Mater.* 10 (1998) 1049–1053;
(b) S. Mikoshiba, S. Hayase, *J. Mater. Chem.* 9 (1999) 591–598;
(c) C.V. Nguyen, K.R. Carter, C.J. Hawker, J.L. Hedrick, R.L. Jaffe, R.D. Miller, J.F. Remenar, H.W. Rhee, P.M. Rice, M.F. Toney, M. Trollsas, D.Y. Yoon, *Chem. Mater.* 11 (1999) 3080–3085.
[33] (a) B.D. Hatton, K. Landskron, W. Whitnall, D.D. Perovic, G.A. Ozin, *Adv. Funct. Mater.* 15 (2005) 823–829;
(b) M.C. Tanese, D. Fine, A. Dodabalapur, L. Torsi, *Microelectron. J.* 37 (2006) 837–840;
(c) B.D. Hatton, K. Landskron, W.J. Hunks, M.R. Bennett, D. Shukaris, D.D. Perovic, G.A. Ozin, *Mater. Today* 9 (2006) 22–31.
[34] B.D. Hatton, K. Landskron, W. Whitnall, D.P. Perovic, G.A. Ozin, *Adv. Funct. Mater.* 15 (2005) 823–829.
[35] T. Nakano, K. Tokunaga, T. Ohta, *J. Electrochem. Soc.* 142 (1995) 1303–1308.
[36] (a) B.J. Cha, S. Kim, K. Char, J.-K. Lee, D.Y. Yoon, H.-W. Rhee, *Chem. Mater.* 18 (2006) 378–385;
(b) B.J. Cha, J.M. Yang, *J. Appl. Polym. Sci.* 104 (2007) 2906–2912.
[37] (a) C.-M. Leu, G.M. Reddy, K.H. Wei, C.F. Shu, *Chem. Mater.* 15 (2003) 2261–2265;
(b) C.-M. Leu, Y.-T. Chang, K.H. Wei, *Chem. Mater.* 15 (2003) 3721–3727;
(c) C.-M. Leu, Y.-T. Chang, K.H. Wei, *Macromolecules* 36 (2003) 9122–9127.
[38] A. Kowalewska, W. Fortuniak, K. Różga-Wijas, B. Handke (in preparation).
[39] G. Lapienis, B. Wiktorska, *J. Polym. Sci. Part A Polym. Chem.* 46 (2008) 3869–3875.
[40] R.L. Merker, M.J. Scott, *J. Am. Chem. Soc.* 85 (1963) 2243–2244.
[41] D. Perrin, W.L.F. Armarego, in: *Purification of Laboratory Chemicals*, Pergamon Press, Oxford, 1980.